International Journal of Control, Automation and Systems 14(1) (2016) 163-173
http://dx.doi.org/10.1007/s12555-015-2004-9

ISSN:1598-6446 eISSN:2005-4092
http://www.springer.com/12555

Distance-based Acyclic Minimally Persistent Formations with Non-steepest Descent Control

Myoung-Chul Park and Hyo-Sung Ahn*

Abstract: In this paper, we propose a control law to maneuver a group of mobile autonomous agents in the plane, where the information architecture among the agents is modeled by a directed graph. The objective is to achieve a prescribed formation shape by adjusting the inter-agent distances only, which is called the distance-based formation control. The proposed control law uses only relative position measurements so that each agent achieves its control objective in a decentralized manner. On the basis of the proposed control law, we analyze the convergence property of squared-distance errors. We first study a triangular formation and then extend the results of to acyclic minimally persistent formations having more than three agents. We also examine the formation including a moving leader. Numerical simulations and experiments with mobile robot platform are included.

Keywords: Decentralized control, formation control, graph rigidity, persistent formation.

1. INTRODUCTION

In recent years, there have been many publications on the formation control of multi-agent systems [1–18]. Depending on the variables that are sensed and controlled, the formation control problems are categorized into several parts [15]. Two major approaches to control the shape of formations are the displacement-based control and the distance-based control. In the displacement-based control, each agent is supposed to maintain the prescribed relative position(s) to its neighbor(s). In this case, it is required for each agent to have a common directional reference frame. On the other hand, in the distance-based formation control, each agent is supposed to maintain the inter-agent distances without the necessity of the common reference frame. In that regard, the distance-based formation control reflects more general distributed systems, but the loss of common directional sense makes the implementation of the control law and the analysis on the motion of the agents much more complicated.

To maintain a specific formation shape by means of inter-agent distance control, it is necessary to introduce the notion of graph rigidity [4, 19]. Suppose that the vertices of the graph in Fig. 1 represent mobile agents, and the edges between the vertices represent the inter-agent distances. In two-dimensional space, while the shape of the formation in Fig. 1(b) cannot be deformed by a continuous motion preserving the inter-agent distances, the formation in Fig. 1(a) may change even if every inter-agent distance is constant. Moreover, certain formations represented by directed graphs undergo continuous deformation even if the underlying graphs are rigid. This interesting phenomenon is explored by Hendrickx *et al.* [20]. Hendrickx *et al.* extend the notion of (generic) graph rigidity to the case of directed graphs, which leads a concept of persistence playing an important role in the directed formation control. Yu *et al.* introduce the extension of persistence from two-dimensional space to n-dimensional space [21]. Persistence is a combined notion of rigidity and constraint consistence. More rigorous definitions and properties on persistence are found in [20, 21].

Although rigidity or persistence could be necessary conditions to solve the formation control problems, they do not provide a practical control law.

A remarkable control strategy is the gradient descent control. Krick *et al.* use the gradient control law to achieve

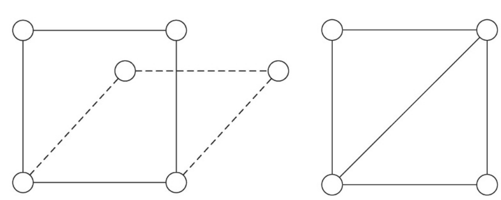

(a) A flexible framework. (b) A rigid framework.

Fig. 1. Examples of flexible and rigid frameworks.

Manuscript received October 18, 2015; revised December 22, 2015; accepted December 30, 2015. Recommended by Guest Editors PooGyeon Park and Ju H. Park. This research is supported by Ministry of Culture, Sports and Tourism(MCST) and Korea Creative Content Agency(KOCCA) in the Culture Technology(CT) Research & Development Program. The authors appreciate the reviewers for their constructive comments and suggestions.

Myoung-Chul Park and Hyo-Sung Ahn are with the School of Mechatronics, Gwangju Institute of Science and Technology (GIST), 123 Cheomdangwagi-ro(Oryong-dong), Buk-gu, Gwangju 61005, Korea (e-mails: {mcpark, hyosung}@gist.ac.kr).
* Corresponding author.

local asymptotic stability of infinitesimally rigid undirected formations. Their results are induced from the center manifold theory, and extended to directed formations, but the results are limited only for acyclic minimally persistent formations satisfying certain conditions [7]. Yu *et al*. and Summers *et al*. achieve local asymptotic stability of minimally persistent formations not restricted to be acyclic [8, 12]. Oh and Ahn propose another novel control strategy that directly control the inter-agent distance dynamics [11].

In this paper, we propose a control law which is a generalized type of the gradient control law used in the literature [2, 5, 9, 10]. The control law proposed in [2, 5, 9, 10] is a kind of steepest descent method used to minimize the objective function. Thus, the basic idea to achieve the desired formation shape is to minimize the error from the desired formation shape. Obviously, the optimization method may not be necessary to seek the steepest descent direction, so we are going to show that more general optimization strategy including non-steepest direction can be used to achieve the desired formation shape also. Unlike [2, 5, 9, 10] dealing with only triangular formations, we can achieve the desired formation shape characterized by acyclic minimally persistent formations consisting of N agents. We also implement the proposed control law to a group of two wheeled-mobile robots to show the validity of the control law.

The rest of the paper is organized as follows. In Section 2, we provide some background knowledge of graph theory and explain the motion of the agents. The problem we want to solve is addressed in this section. Next, we analyze a basic triangular formation, and explain our results in Section 3. In Section 4, we extend our results from 3-agent acyclic triangular formation to N-agent acyclic minimally persistent formations with $N \geq 4$. In Section 5, we consider a formation with moving leader. Simulations and experiments verifying our results are contained in Section 6, and the final conclusion is in Section 7.

2. PRELIMINARIES

The set of positive real numbers is denoted by $\mathbb{R}_{>0}$. For a given finite set $\mathcal{A}$, $|\mathcal{A}|$ denotes the number of elements of $\mathcal{A}$. For a given square matrix A, trace$A$ means the sum of all elements in the main diagonal. We use $0_{n\times n}$ and I_n to represent the n by n zero matrix and the identity matrix, respectively. For a given vector $\mathbf{v}$, $\|\mathbf{v}\|$ denotes the Euclidean norm of $\mathbf{v}$. We use $\mathbf{0}$ to represent the zero vector with an appropriate dimension depending on the corresponding equations. For two scalar functions $f(x)$ and $g(x)$, $f(x) \in \Theta(g(x))$ means that there exist positive constants c_1, c_2, and k such that $c_1 \leq |f(x)| \leq c_2|g(x)|$ for all $x \geq k$.

2.1. Graph representation and acyclic minimally persistent formation

A directed graph $\mathcal{G} = (\mathcal{V}, \mathcal{E})$ consists of two sets of vertices (agents) and edges. Thus, $\mathcal{V} = \{1, \ldots, N\}$ is the set of vertices, and $\mathcal{E} = \{\ldots, (i, j), \ldots\} \subseteq \mathcal{V} \times \mathcal{V}$ is the set of edges. An edge (i, j) denotes the unique connection joining two vertices i and j. We use (i, j) if the edge leaves vertex j and enters vertex i. We assume that there is no self loop, i.e., $(i, i) \notin \mathcal{E}$ for all $i \in \mathcal{V}$ and there are no multiple edges joining any two of the vertices. Additionally, we assume that the given directed graph is *acyclic* thus there is no sequence of edges $(v_1, v_2), (v_2, v_3), \ldots, (v_{k-2}, v_{k-1}), (v_{k-1}, v_k)$ such that $v_1 = v_k$. If we consider $\mathcal{G}$ as an undirected graph, then the direction of each edge does not have meaning, so the edge joining two vertices denotes the bidirectional connection between them. The set of neighbors of vertex i is defined as $\mathcal{N}_i = \{j \in \mathcal{V} \colon (j, i) \in \mathcal{E}\}$. Let $\mathbf{p}_i \in \mathbb{R}^n$ denote the position vector of vertex i in $\mathbb{R}^n$ for each $i \in \mathcal{V}$. Then, we call $\mathbf{p} = [\mathbf{p}_1^\top \ \ldots \ \mathbf{p}_{|\mathcal{V}|}^\top]^\top \in \mathbb{R}^{n|\mathcal{V}|}$ a *realization* of $\mathcal{G}$ in $\mathbb{R}^n$. A pair of graph and its realization is called a *framework*, which is denoted by $(\mathcal{G}, \mathbf{p})$.

For a given directed graph $\mathcal{G}$ and two different realizations $\mathbf{p}$ and $\mathbf{q}$, two frameworks $(\mathcal{G}, \mathbf{p})$ and $(\mathcal{G}, \mathbf{q})$ are said to be *equivalent* if

$$\|\mathbf{p}_i - \mathbf{p}_j\| = \|\mathbf{q}_i - \mathbf{q}_j\|, \quad \forall (i, j) \in \mathcal{E}.$$

Two realizations $\mathbf{p}$ and $\mathbf{q}$ are said to be *congruent* if

$$\|\mathbf{p}_i - \mathbf{p}_j\| = \|\mathbf{q}_i - \mathbf{q}_j\|, \quad \forall i, j \in \mathcal{V}.$$

For a given distance set $\mathcal{L} = \{d_{ij} \in \mathbb{R}_{>0} \colon (i, j) \in \mathcal{E}\}$, we say $\mathbf{p}_j$ is *fitting* for $\mathcal{L}$ if there is no other point for $\mathbf{p}_j$, which is defined as $\mathbf{p}'_j$, such that

$$\begin{aligned}&\{(i, j) \in \mathcal{E} \colon \|\mathbf{p}_i - \mathbf{p}_j\| = d_{ij}\} \\ &\subsetneq \left\{(i, j) \in \mathcal{E} \colon \|\mathbf{p}_i - \mathbf{p}'_j\| = d_{ij}\right\}.\end{aligned}$$

If, $\forall j \in \mathcal{V}$, $\mathbf{p}_j$ is fitting for $\mathcal{L}$, then we say $\mathbf{p}$ is a fitting realization for $\mathcal{L}$.

Definition 1 Hendrickx *et al*. [20]**:** For a given framework $(\mathcal{G}, \mathbf{p})$ in $\mathbb{R}^2$, let $\mathcal{L}$ be a set of distances given by $\mathcal{L} = \{d_{ij} \colon d_{ij} = \|\mathbf{p}_i - \mathbf{p}_j\|, (i, j) \in \mathcal{E}\}$. The framework $(\mathcal{G}, \mathbf{p})$ is *persistent* in $\mathbb{R}^2$ if there exists ε such that every realization $\mathbf{p}' \in \mathbb{R}^{2|\mathcal{V}|}$ fitting for $\mathcal{L}$ and satisfying $d(\mathbf{p}, \mathbf{p}') < \varepsilon$ is congruent to $\mathbf{p}$, where $d(\mathbf{p}, \mathbf{p}') = \max_{i\in\mathcal{V}} \|\mathbf{p}_i - \mathbf{p}'_i\|$. If $(\mathcal{G}, \mathbf{p})$ is persistent for almost all realizations of $\mathcal{G}$, then $\mathcal{G}$ is *generically persistent*.

Definition 2: A persistent graph is *minimally persistent* if none of the edges can be removed without loosing persistence.

Now, we characterize acyclic minimally persistent graphs via Theorems 4 and 5 in [20].

Theorem 1 Combination of Theorems 4 and 5 in [20]**:** An acyclic graph having more than one vertex is (generically) minimally persistent in $\mathbb{R}^2$ if and only if

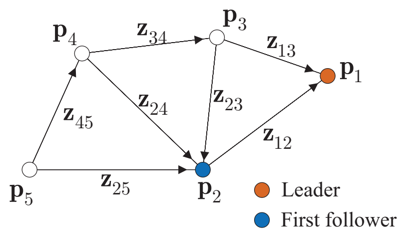

Fig. 2. An acyclic minimally persistent formation consisting of five-agents.

- One vertex (called the leader) has an out-degree 0.
- One vertex (called the first follower) has an out-degree 1 and the corresponding edge is incident to the leader.
- Every other vertex has an out-degree 2.

These conditions are equivalent to Corollary 2 in [20]. An example of acyclic minimally persistent graph is illustrated in Fig. 2.

2.2. Behavior of the group of agents

We use $\mathbf{p}_i(t) \in \mathbb{R}^2$ to represent the position vector of agent i at time t based on the Cartesian coordinate system. Our aim is to maneuver the shape of the formation produced by the mobile agents only by controlling some inter-agent distances between the agents. For a given formation graph $\mathcal{G} = (\mathcal{V}, \mathcal{E})$, if $(i, j) \in \mathcal{E}$, it means that agent j is responsible for maintaining the desired distance to agent i. We assume that the motion of each agent is modeled by a single integrator. Thus, we have

$$\dot{\mathbf{p}}_i = \mathbf{u}_i, \quad \forall i \in \mathcal{V}, \tag{1}$$

where $\mathbf{u}_i \in \mathbb{R}^2$ is the control input for agent i. For convenience, we define the relative displacement corresponding to (i, j) as

$$\mathbf{z}_{ij}(t) = \mathbf{p}_i(t) - \mathbf{p}_j(t), \quad \forall (i, j) \in \mathcal{E}. \tag{2}$$

Each agent is assumed to be able to measure the relative displacement(s) to their neighbor(s).

The problem we want to solve is given in the following statements.

Problem 1: Let us assume that the formation graph of the group of N agents, whose motion is described by (1), is given by an acyclic minimally persistent graph $\mathcal{G} = (\mathcal{V}, \mathcal{E})$. For a given desired realization $\mathbf{p}^* \in \mathbb{R}^{2|\mathcal{V}|}$, design a decentralized control law that only uses the relative measurements in (2) to make $\mathbf{p}(t)$ converge to a point congruent to $\mathbf{p}^*$.

3. BASIC TRIANGULAR FORMATION

First, we consider the group of three mobile agents. By assigning indices 1,2 and 3 to the leader, the first follower and the rest, respectively, the formation graph is depicted as Fig. 3. Thus, we have $\mathcal{G} = (\mathcal{V}, \mathcal{E})$, where $\mathcal{V} = \{1, 2, 3\}$, and $\mathcal{E} = \{(1, 2), (1, 3), (2, 3)\}$. To guarantee the triangular formation, we assume that $\|\mathbf{p}_i^* - \mathbf{p}_j^*\| \neq 0$ for all $(i, j) \in \mathcal{E}$, and

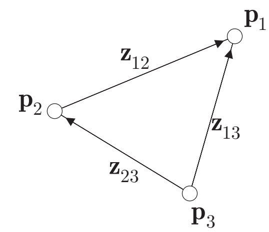

Fig. 3. A three-agent acyclic formation.

$$\|\mathbf{p}_1^* - \mathbf{p}_2^*\| < \|\mathbf{p}_1^* - \mathbf{p}_3^*\| + \|\mathbf{p}_2^* - \mathbf{p}_3^*\|, \tag{3}$$
$$\|\mathbf{p}_1^* - \mathbf{p}_3^*\| < \|\mathbf{p}_1^* - \mathbf{p}_2^*\| + \|\mathbf{p}_2^* - \mathbf{p}_3^*\|, \tag{4}$$
$$\|\mathbf{p}_2^* - \mathbf{p}_3^*\| < \|\mathbf{p}_1^* - \mathbf{p}_2^*\| + \|\mathbf{p}_1^* - \mathbf{p}_3^*\|. \tag{5}$$

We should design controllers so that

$$\lim_{t \to \infty} \|\mathbf{p}_i(t) - \mathbf{p}_j(t)\| = \|\mathbf{p}_i^* - \mathbf{p}_j^*\|, \quad \forall i, j \in \mathcal{V}.$$

We define the desired formation $\mathcal{D}_{\mathbf{p}^*}$ as the set of all realizations which are congruent to $\mathbf{p}^*$, i.e.,

$$\mathcal{D}_{\mathbf{p}^*} = \left\{ \mathbf{p} \in \mathbb{R}^{2|\mathcal{V}|} : \|\mathbf{p}_i - \mathbf{p}_j\| = \|\mathbf{p}_i^* - \mathbf{p}_j^*\|, \forall i, j \in \mathcal{V} \right\}.$$

Since the formation is triangular, the shape of the formation is uniquely determined by the length of the edges. Thus, the desired formation can be defined in terms of the edge length as follows:

$$\mathcal{D}'_{\mathbf{p}^*} = \left\{ \mathbf{p} \in \mathbb{R}^{2|\mathcal{V}|} : \|\mathbf{p}_i - \mathbf{p}_j\| = \|\mathbf{p}_i^* - \mathbf{p}_j^*\|, \forall (i, j) \in \mathcal{E} \right\}.$$

We define the squared-distance errors corresponding to each edge as

$$e_{ij}(t) = \|\mathbf{p}_i(t) - \mathbf{p}_j(t)\|^2 - \|\mathbf{p}_i^* - \mathbf{p}_j^*\|^2, \quad \forall (i, j) \in \mathcal{E}. \tag{6}$$

Then, we define the local potential function of agent i as

$$\phi_i(\mathbf{p}(t)) = \begin{cases} k_\phi \sum\limits_{j \in \mathcal{N}_i} e_{ji}^2 & \text{if } |\mathcal{N}_i| \geq 1, \\ 0 & \text{if } |\mathcal{N}_i| = 0, \end{cases} \quad \forall i \in \mathcal{V}, \tag{7}$$

where k_ϕ is a positive constant. Thus, we can achieve the desired formation by designing controllers that make $\phi_i(\mathbf{p}(t)) \to 0$ as t goes to infinity.

3.1. Modified gradient control law

A typical control law used in the literature to maneuver the directed formations is give by

$$\mathbf{u}_i = -\left[\frac{\partial \phi_i}{\partial \mathbf{p}_i}\right]^\top, \quad \forall i \in \mathcal{V}, \tag{8}$$

For example, Cao *et al.* use (8) for three-agent case in [2, 5], and Krick *et al.* use (8) for N-agent acyclic minimally persistent formations [7, Section 7]. According to

Cao *et al.*, the three-agent acyclic formation exponentially converges to the desired formation if the initial locations of the agents are not collinear.

The control law in (8) is sometimes called the *steepest descent method* in optimization, which reflects the steepest descent direction of the objective function. Thus, the basic idea contained in (8) is to move each agent to minimize the distance error along the steepest descent direction. However, it is not necessary to seek the steepest descent direction. We can generalize (8) so that the direction of the control input vector heads for any descent direction. In that regard, we propose a modified control law given by

$$\mathbf{u}_i = \begin{cases} -\left[\dfrac{\partial \phi_i}{\partial \mathbf{p}_i}\right]^\top & \text{if } |\mathcal{N}_i| \leq 1, \\ -Q\left[\dfrac{\partial \phi_i}{\partial \mathbf{p}_i}\right]^\top & \text{if } |\mathcal{N}_i| \geq 2, \end{cases} \quad \forall i \in \mathcal{V}, \tag{9}$$

where

$$Q = \begin{bmatrix} \cos\theta & -\sin\theta \\ \sin\theta & \cos\theta \end{bmatrix}, \tag{10}$$

with a constant θ such that $0 < \cos\theta \leq 1$. For convenience, we let $k_\phi = 1/4$ in (7). Then, the control law in (9) is written in detail as

$$\mathbf{u}_1 = \mathbf{0}, \quad \mathbf{u}_2 = e_{12}\mathbf{z}_{12}, \quad \mathbf{u}_3 = Q(e_{13}\mathbf{z}_{13} + e_{23}\mathbf{z}_{23}). \tag{11}$$

Thus, the state equation of relative position vectors can be obtained as

$$\dot{\mathbf{z}}_{12} = -e_{12}\mathbf{z}_{12}, \tag{12}$$
$$\dot{\mathbf{z}}_{13} = -Q(e_{13}\mathbf{z}_{13} + e_{23}\mathbf{z}_{23}), \tag{13}$$
$$\dot{\mathbf{z}}_{23} = e_{12}\mathbf{z}_{12} - Q(e_{13}\mathbf{z}_{13} + e_{23}\mathbf{z}_{23}), \tag{14}$$

and written by

$$\dot{\mathbf{z}} = \mathbf{f}(\mathbf{z}), \quad \mathbf{z}(0) = \mathbf{z}_0, \tag{15}$$

where $\mathbf{z} = [\mathbf{z}_{12}^\top \;\; \mathbf{z}_{13}^\top \;\; \mathbf{z}_{23}^\top]^\top \in \mathbb{R}^{2|\mathcal{E}|}$. The solution of (15) will be denoted by $\mathbf{z}(t, \mathbf{z}_0)$, $\mathbf{z}(t)$ or simply $\mathbf{z}$.

We are going to investigate (15) to know whether or not the length of edges converge to 0. The equilibrium set of (15) is partitioned into the desired and incorrect equilibrium subsets. Remark that $\|\mathbf{z}_{12}\|$ and e_{12} cannot be 0 simultaneously because $\|\mathbf{p}_1^* - \mathbf{p}_2^*\| \neq 0$. If $\mathbf{z}_{12} = \mathbf{0}$ and $e_{12} \neq 0$, then $\mathbf{z}_{13} = \mathbf{z}_{23}$. Thus, two subsets of the equilibrium set are defined by

$$\mathcal{U}_1 = \left\{\mathbf{z} \in \mathbb{R}^{2|\mathcal{E}|} \colon \mathbf{z}_{12} = \mathbf{z}_{13} = \mathbf{z}_{23} = \mathbf{0}\right\},$$
$$\mathcal{U}_2 = \left\{\mathbf{z} \in \mathbb{R}^{2|\mathcal{E}|} \colon \mathbf{z}_{12} = \mathbf{0},\, \mathbf{z}_{13} = \mathbf{z}_{23},\, e_{13} + e_{23} = 0\right\}.$$

If $\mathbf{z}_{12} \neq \mathbf{0}$ and $e_{12} = 0$, we have equilibrium subsets defined by

$$\mathcal{U}_3 = \{\mathbf{z} \in \mathbb{R}^{2|\mathcal{E}|} \colon \mathbf{z}_{12} = \mathbf{z}_{13} - \mathbf{z}_{23},\, e_{12} = 0,\; e_{13}\mathbf{z}_{13} + e_{23}\mathbf{z}_{23} = \mathbf{0},\, e_{13} \text{ or } e_{23} \neq 0\},$$

$$\mathcal{D}_{\mathbf{z}^*} = \left\{\mathbf{z} \in \mathbb{R}^{2|\mathcal{E}|} \colon \mathbf{z}_{12} = \mathbf{z}_{13} - \mathbf{z}_{23},\, e_{12} = e_{13} = e_{23} = 0\right\}.$$

If we use $\mathcal{W}$ to denote the equilibrium set of (15), i.e., $\mathcal{W} = \{\mathbf{z} \in \mathbb{R}^{2|\mathcal{E}|} \colon \mathbf{f}(\mathbf{z}) = \mathbf{0}\}$, then $\mathcal{W}$ is partitioned into $\mathcal{U}$ and $\mathcal{D}_{\mathbf{z}^*}$, where $\mathcal{U} = \mathcal{U}_1 \cup \mathcal{U}_2 \cup \mathcal{U}_3$.

Note that $\mathbf{p} \in \mathcal{D}'_{\mathbf{p}^*}$ if and only if $\mathbf{z} \in \mathcal{D}_{\mathbf{z}^*}$. Therefore, by investigating stability of $\mathcal{D}_{\mathbf{z}^*}$, we can analyze stability of $\mathcal{D}'_{\mathbf{p}^*}$.

3.2. Analysis

From (12)–(14), it is apparent that $\mathbf{z}_{13}$ and $\mathbf{z}_{23}$ do not affect (12). Therefore, (12) can be solved solely. From the fact that $e_{12} = \|\mathbf{z}_{12}\|^2 - \|\mathbf{p}_1^* - \mathbf{p}_2^*\|^2$ and $\dot{e}_{12} = 2\mathbf{z}_{12}^\top\dot{\mathbf{z}}_{12}$, by multiplying both side of (12) by $\mathbf{z}_{12}^\top$, we have

$$\mathbf{z}_{12}^\top\dot{\mathbf{z}}_{12} = -e_{12}\|\mathbf{z}_{12}\|^2 \Leftrightarrow \frac{1}{2}\dot{e}_{12} = -e_{12}(e_{12} + d_{12}^2),$$

where $d_{ij} = \|\mathbf{p}_i^* - \mathbf{p}_j^*\|$ for all $i, j \in \mathcal{V}$. For every initial condition $e_{12}(0) \in (-d_{12}^2, \infty)$, the solution of this first-order ordinary differential equation is given by

$$e_{12} = \frac{\pm\gamma d_{12}^2 \exp(-2d_{12}^2 t)}{1 \mp \gamma \exp(-2d_{12}^2 t)}, \tag{16}$$

where $\gamma = e_{12}(0)/(e_{12}(0) + d_{12}^2)$. Therefore, we know that e_{12} and $\|\dot{\mathbf{z}}_{12}\|$ are bounded by an exponentially decaying function. If agents 1 and 2 are collocated from the beginning, i.e., $\mathbf{z}_{12}(0) = \mathbf{0}$, then $\mathbf{z}(t) = \mathbf{0}$ for all $t \geq 0$ from (12).

To investigate convergence of e_{13} and e_{23}, let

$$V_3(\mathbf{z}(t)) = \phi_3(\mathbf{p}(t)) = \frac{1}{4}(e_{13}^2 + e_{23}^2).$$

Then, we have

$$\begin{aligned}\dot{V}_3 &= \frac{1}{2}(e_{13}\dot{e}_{13} + e_{23}\dot{e}_{23}) \\ &= e_{13}\mathbf{z}_{13}^\top\dot{\mathbf{z}}_{13} + e_{23}\mathbf{z}_{23}^\top\dot{\mathbf{z}}_{23} \\ &= e_{13}\mathbf{z}_{13}^\top(\mathbf{0} - Q(e_{13}\mathbf{z}_{13} + e_{23}\mathbf{z}_{23})) \\ &\quad + e_{23}\mathbf{z}_{23}^\top(e_{12}\mathbf{z}_{12} - Q(e_{13}\mathbf{z}_{13} + e_{23}\mathbf{z}_{23})) \\ &= -e_{13}^2\mathbf{z}_{13}^\top Q\mathbf{z}_{13} - e_{13}e_{23}\mathbf{z}_{13}^\top(Q + Q^\top)\mathbf{z}_{23} \\ &\quad - e_{23}^2\mathbf{z}_{23}^\top Q\mathbf{z}_{23} + e_{23}e_{12}\mathbf{z}_{23}^\top\mathbf{z}_{12}.\end{aligned}$$

From the facts that $\mathbf{z}_{ij}^\top Q\mathbf{z}_{ij} = \cos\theta\|\mathbf{z}_{ij}\|^2$, and

$$Q + Q^\top = \begin{bmatrix} 2\cos\theta & 0 \\ 0 & 2\cos\theta \end{bmatrix},$$

we have

$$\begin{aligned}\dot{V}_3 &= -\cos\theta(e_{13}^2\|\mathbf{z}_{13}\|^2 + 2e_{13}e_{23}\mathbf{z}_{13}^\top\mathbf{z}_{23} + e_{23}^2\|\mathbf{z}_{23}\|^2) \\ &\quad + e_{23}e_{12}\mathbf{z}_{23}^\top\mathbf{z}_{12} \\ &= -\cos\theta\underbrace{\|e_{13}\mathbf{z}_{13} + e_{23}\mathbf{z}_{23}\|^2}_{\triangleq g(\mathbf{z}(t))} + \underbrace{e_{23}e_{12}\mathbf{z}_{23}^\top\mathbf{z}_{12}}_{\triangleq h(\mathbf{z}(t))}.\end{aligned} \tag{17}$$

Lemma 1: The squared-distance errors e_{13} and e_{23} are bounded.

Proof: We already know that e_{12} converges to 0 from the given initial condition. Let us assume that e_{13} and e_{23} diverge to $+\infty$ as time goes on. Since $\mathbf{z}_{13} = \mathbf{z}_{12} + \mathbf{z}_{23}$, and e_{ij} is defined by (6), $e_{13} \simeq e_{23} \simeq \|\mathbf{z}_{13}\|^2 \simeq \|\mathbf{z}_{23}\|^2$ for large enough e_{13} and e_{23}.[1] Therefore, we see that $g \in \Theta(e_{12}^3)$, and that $h \in \Theta(e_{13}\sqrt{e_{13}})$, which means that $\dot{V}_3$ becomes negative as e_{13} and e_{23} increase. Thus, V_3 is bounded, and the boundedness of e_{13} and e_{23} is clear from the boundedness of V_3. □

From the boundedness of e_{13} and e_{23}, boundedness of $\mathbf{z}_{13}$ and $\mathbf{z}_{23}$ are evident. Thus, h is bounded by an exponentially decaying function. Now, by taking integration of $\dot{V}_3$, we have

$$\begin{aligned} &V_3(\mathbf{z}(t,\mathbf{z}_0)) - V_3(\mathbf{z}(0,\mathbf{z}_0)) = \\ &\quad -\cos\theta \int_0^t g(\mathbf{z}(s,\mathbf{z}_0))\,\mathrm{d}s + \int_0^t h(\mathbf{z}(s,\mathbf{z}_0))\,\mathrm{d}s. \end{aligned} \tag{18}$$

Theorem 2: The relative displacement, $\mathbf{z}$ converges to $\mathcal{U}_3$ or $\mathcal{D}_{\mathbf{z}^*}$ if $\mathbf{z}_{12}(0) \neq \mathbf{0}$. Moreover, if $\mathbf{z}$ converges to $\mathcal{D}_{\mathbf{z}^*}$ with V_3 converging to 0, then convergence rate is locally exponential.

Proof: First, we know that $h(\mathbf{z}(t,\mathbf{z}_0))$ is bounded by an exponentially decaying function. Thus, $\int_0^t h(\mathbf{z}(s,\mathbf{z}_0))\,\mathrm{d}s$ converges to a constant. Since the first integral in the right side of (18) is monotonically decreasing as t increases, the integral must converge to a constant due to the boundedness of V_3. Next, the uniform continuity of $g(\mathbf{z}(t,\mathbf{z}_0))$ can be revealed by showing that $\dot{g}$ is bounded and then Barbalat's lemma[2] concludes that $\lim_{t\to\infty} g(\mathbf{z}(t,\mathbf{z}_0)) = 0$. As a result, $\|e_{13}\mathbf{z}_{13} + e_{23}\mathbf{z}_{23}\|$ converges to $\mathbf{0}$ as time goes to infinity. Since $\mathbf{z}_{13}$ and $\mathbf{z}_{23}$ exist in $\mathbb{R}^2$, either e_{13} and e_{23} converge to 0 with linearly independent $\mathbf{z}_{13}$ and $\mathbf{z}_{23}$ or $e_{13}\mathbf{z}_{13} + e_{23}\mathbf{z}_{23}$ converges to $\mathbf{0}$ with at least nonzero one of e_{13} and e_{23}. We already know that e_{12} converges to 0 if $\mathbf{z}_{12} \neq \mathbf{0}$. Therefore, $\mathbf{z}$ finally converges to $\mathcal{U}_3$ or $\mathcal{D}_{\mathbf{z}^*}$.

Now, let us assume that $\mathbf{z}$ converges to $\mathcal{D}_{\mathbf{z}^*}$. To prove the exponential convergence rate, define $\Omega(r)$ as

$$\left\{\mathbf{z} \in \mathbb{R}^{2|\mathcal{E}|} : e_{12}^2 + e_{13}^2 + e_{23}^2 \le r^2\right\}.$$

Then, from (3)–(5), there exist $t_\varepsilon, r_\varepsilon \in \mathbb{R}_{>0}$ such that $\mathbf{z}_{13}$ and $\mathbf{z}_{23}$ are linearly independent in $\Omega(r_\varepsilon)$ and $\mathbf{z}(t,\mathbf{z}_0) \in \Omega(r_\varepsilon)$ for each $t \ge t_\varepsilon$. Remark that $\mathcal{D}_{\mathbf{z}^*} \subsetneq \Omega(r_\varepsilon)$. From the Cauchy–Schwarz inequality, it is true that $\mathbf{z}_{13}^\top \mathbf{z}_{23} < \|\mathbf{z}_{13}\|\|\mathbf{z}_{23}\|$ for all $\mathbf{z} \in \Omega(r_\varepsilon)$. Now, there exists $\rho : \mathbb{R} \to [0,1)$ such that

$$\begin{aligned} g &= e_{13}^2\|\mathbf{z}_{13}\|^2 + 2e_{13}e_{23}\mathbf{z}_{13}^\top\mathbf{z}_{23} + e_{23}^2\|\mathbf{z}_{23}\|^2 \\ &\ge e_{13}^2\|\mathbf{z}_{13}\|^2 - 2\rho^2(t)|e_{13}||e_{23}|\|\mathbf{z}_{13}\|\|\mathbf{z}_{23}\| + e_{23}^2\|\mathbf{z}_{23}\|^2 \\ &= (1-\rho^2(t))e_{13}^2\|\mathbf{z}_{13}\|^2 + (1-\rho^2(t))e_{23}^2\|\mathbf{z}_{23}\|^2 \\ &\quad + \rho^2(t)e_{13}^2\|\mathbf{z}_{13}\|^2 - 2\rho^2(t)|e_{13}||e_{23}|\|\mathbf{z}_{13}\|\|\mathbf{z}_{23}\| \\ &\quad + \rho^2(t)e_{23}^2\|\mathbf{z}_{23}\|^2 \\ &\ge \min\left\{\inf_{\mathbf{z}\in\Omega(r_\varepsilon)}\|\mathbf{z}_{13}\|^2, \inf_{\mathbf{z}\in\Omega(r_\varepsilon)}\|\mathbf{z}_{23}\|^2\right\} \\ &\quad \times \left[\inf_{t\in[t_\varepsilon,\infty)}(1-\rho^2(t))\right](e_{13}^2 + e_{23}^2) \\ &= k_g V_3, \end{aligned}$$

for all $t \ge t_\varepsilon$. Since $\mathbf{z}$ converges to $\mathcal{D}_{\mathbf{z}^*}$ as $t \to \infty$, we can restrict $\rho(t)$ so that $\lim_{t\to\infty}\rho^2(t) = k_\rho < 1$, which results in that $\inf_{t\in[t_\varepsilon,\infty)}(1-\rho^2(t)) > 0$ and $k_g > 0$. Thus, from (17), we have

$$\dot{V}_3 \le h - k_g\cos\theta V_3.$$

From the fact that h is bounded by an exponentially decaying function, we can conclude that V_3 is bounded by an exponentially decaying function via the comparison lemma [22, Lemma 3.4], and we achieve locally exponential convergence rate. □

From Theorem 2, we have two cases. Convergence of $\mathbf{z}$ to $\mathcal{D}_{\mathbf{z}^*}$ is desired. We are going to show that $\mathcal{U}_3$ is unstable via linearization method. Consider the linearization of (15) about $\mathcal{U}_3$. Since $e_{12} = 0$ in $\mathcal{U}_3$, the Jacobian $J_\mathbf{f}$ is given by

$$\begin{aligned} J_\mathbf{f} &= \frac{\partial \mathbf{f}(\mathbf{z})}{\partial \mathbf{z}} \\ &= \begin{bmatrix} -Z_{12} & 0_{2\times2} & 0_{2\times2} \\ 0_{2\times2} & -Q(Z_{13}+e_{13}I_2) & -Q(Z_{23}+e_{23}I_2) \\ Z_{12} & -Q(Z_{13}+e_{13}I_2) & -Q(Z_{23}+e_{23}I_2) \end{bmatrix}, \end{aligned}$$

where $Z_{ij} = 2\mathbf{z}_{ij}\mathbf{z}_{ij}^\top$. From the shape of $J_\mathbf{f}$, we know that the eigenvalues of $J_\mathbf{f}$ are the eigenvalues of $-Z_{12}$ and $K_\mathbf{f}$, where

$$K_\mathbf{f} = \begin{bmatrix} -Q(Z_{13}+e_{13}I_2) & -Q(Z_{23}+e_{23}I_2) \\ -Q(Z_{13}+e_{13}I_2) & -Q(Z_{23}+e_{23}I_2) \end{bmatrix}.$$

Thus, by investigating the eigenvalues of $K_\mathbf{f}$ and showing that $K_\mathbf{f}$ has eigenvalues whose real parts are strictly positive, we can reach the following statement

Lemma 2: The incorrect equilibrium set $\mathcal{U}_3$ is unstable.

Proof of Lemma 2 is found in Appendix A.

3.3. Analysis of line configuration

An interesting phenomenon observed in the distance-based formation control problem is that there exists an invariant subset in which the agents cannot achieve the desired formation shape. For instance, under the conventional gradient control law used in [2,5,9,10], if the initial locations of the agents are in a line configuration, then the agents cannot escape from the line configuration.

However, if θ in (10) is restricted so that $0 < \cos\theta < 1$, then the line configuration is not invariant anymore. To

[1] Remember that $\|\mathbf{z}_{12}\|$ is ultimately bounded by any given initial condition due to convergence of e_{12}.

[2] If $\lim_{t\to\infty}\varphi(t) = c < \infty$, and $\dot{\varphi}$ is uniformly continuous, then $\lim_{t\to\infty}\dot{\varphi}(t) = 0$.

observe what takes place in our case, define sets $\mathcal{C}_1$, $\mathcal{C}_2$ and $\mathcal{C}$ as

$$\begin{aligned}
\mathcal{C}_1 &= \left\{\mathbf{z} \in \mathbb{R}^{2|\mathcal{E}|} : \mathbf{z}_{12} = \mathbf{0},\ \mathbf{z}_{13} = \mathbf{z}_{23}\right\}, \\
\mathcal{C}_2 &= \Big\{\mathbf{z} \in \mathbb{R}^{2|\mathcal{E}|} : \mathbf{z}_{12} = \mathbf{z}_{13} - \mathbf{z}_{23}, \\
&\qquad\qquad \operatorname{rank}[\mathbf{z}_{13}\ \ \mathbf{z}_{23}] < 2,\ \mathbf{z}_{12} \neq \mathbf{0}\Big\}, \\
\mathcal{C} &= \mathcal{C}_1 \cup \mathcal{C}_2.
\end{aligned}$$

Then, the set of all $\mathbf{z}$ where the formation forms a line configuration is $\mathcal{C}$, and $\mathcal{C}$ is partitioned into $\mathcal{C}_1$ and $\mathcal{C}_2$. If $\mathbf{z}(0) \in \mathcal{C}_1$, then $\mathbf{z}_{12}(t) = \mathbf{0}$ for all $t \geq 0$ as we mentioned in Section 3.2.. Thus, if the agents 1 and 2 are located in the same position from the beginning, we cannot achieve the desired formation using the proposed control law. However, in the case of $\mathcal{C}_2$, we have other possibilities.

Lemma 3: If $0 < \cos\theta < 1$ and $\mathbf{z}(t_a) \in \mathcal{C}_2 \setminus \mathcal{U}_3 = \mathcal{C} \setminus (\mathcal{C}_1 \cup \mathcal{U}_3)$ at a certain t_a, then $\mathbf{z}$ does not stay in $\mathcal{C}$.

Proof: Since $\mathbf{z}_{12} \neq \mathbf{0}$ for all $\mathbf{z} \in \mathcal{C}_2$, $\|\mathbf{z}_{12}\|$ converges to the desired distance d_{12} from (16), so $\mathbf{z}$ does not approach $\mathcal{C}_1$.

If $\mathbf{z}(t_a) \notin \mathcal{U}_3$, then $e_{12}(t_a) \neq 0$ or

$$e_{13}(t_a)\mathbf{z}_{13}(t_a) + e_{23}(t_a)\mathbf{z}_{23}(t_a) \neq \mathbf{0}.$$

In the latter case, $\dot{\mathbf{p}}_3$ is nonzero vector which is not parallel to $\mathbf{z}_{13}(t_a)$ and $\mathbf{z}_{23}(t_a)$ because $\cos\theta < 1$. Thus, agent 3 breaks away from the line configuration (see Fig. 4). If $e_{13}(t_a)\mathbf{z}_{13}(t_a) + e_{23}(t_a)\mathbf{z}_{23}(t_a) = \mathbf{0}$ and $e_{12}(t_a) \neq 0$, then $e_{12}(t)$ converges to zero as $t \to \infty$, which results in nonzero $e_{13}\mathbf{z}_{13} + e_{23}\mathbf{z}_{23}$ so that agent 3 breaks away from the line configuration. Therefore, under the given conditions for Lemma 3, $\mathbf{z}$ does not stay in $\mathcal{C}$. □

Note that Cao *et al.* show that the set $\mathcal{C}$ of collinear agents is positively invariant in the case of $\theta = 0$ [2,5,10], which is a special case such that Q is the identity matrix. In the Cao's paper, the authors characterize exact initial conditions such that the agents achieve the desired formation shape[3]. Lemma 3 means that by choosing an appropriate θ, we can alter $\mathcal{C}$ not to be positively invariant.

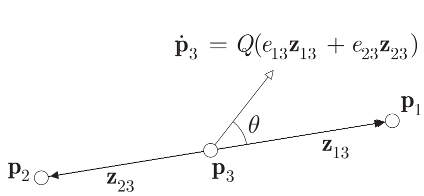

Fig. 4. Control law for $\mathbf{p}_3$ in collinear position.

[3]The agents achieve the desired formation shape under the proposed control law if and only if $\mathbf{z}$ is not in $\mathcal{C}$ at the initial time.

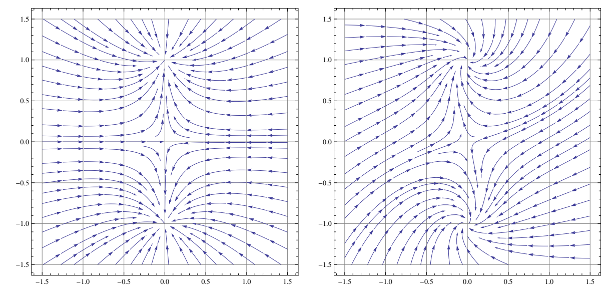

(a) Case: $\theta = 0$. (b) Case: $\theta = \pi/6$.

Fig. 5. Phase portrait with respect to the position of agent 3 provided that agents 1 and 2 do not move.

Theorem 3: For almost every initial condition $\mathbf{z}_0$, the solution trajectory $\mathbf{z}(t, \mathbf{z}_0)$ converges to $\mathcal{D}_{\mathbf{z}^*}$, so the agents achieve the desired formation shape. In particular, almost every line configuration is non-invariant.

Proof: From Lemma 3, if the initial condition of $\mathbf{z}$ is not in $\mathcal{C}_1$ or $\mathcal{U}_3$, then $\mathbf{z}$ breaks away from the line configuration so that $\mathbf{z}_{13}$ and $\mathbf{z}_{23}$ become linearly independent. Thus, the line configuration is not invariant anymore. Moreover, e_{13} and e_{23} converge to zero from Theorem 2 and the subsequent proof. Convergence of e_{12} is already guaranteed, so we can conclude that $\mathbf{z}$ converges to $\mathcal{D}_{\mathbf{z}^*}$. □

Remark that although nonzero θ results in that $\mathcal{C}$ is not invariant, it does not mean that we can get rid of the invariant subset of saddle type. For example, consider $d_{12} = 2$, $d_{13} = d_{23} = \sqrt{2}$, $\mathbf{p}_1(0) = [1\ \ 0]^\top$, $\mathbf{p}_2(0) = [-1\ \ 0]^\top$. Since agent 2 is at the position satisfying the desired distance, agent 2 does not move. In this situation, we can draw a phase portrait with respect to the position of agent 3. Fig. 5(a) shows that the invariant subset of the saddle point is the horizontal axis $\{y = 0\}$. By choosing $\theta = \pi/6$, $\{y = 0\}$ becomes non-invariant, but there still exists another invariant subset of the saddle point. Therefore, choosing $0 < |\theta| < \pi/2$ just transforms the undesired invariant subset.

4. EXTENSION TO GENERAL ACYCLIC MINIMALLY PERSISTENT FORMATIONS

Let us consider an acyclic minimally persistent graph $\mathcal{G}$ such that $\mathcal{V} = \{1, \ldots, N\}$, $N > 3$, $\mathcal{E} = \{\ldots, (i,j), \ldots\}$, $|\mathcal{E}| = 2N - 3$. We assume that agent 1 is the leader, agent 2 is the first follower, and every neighbor of agent i has an index smaller than i for all $i \in \{3, \ldots, N\}$. From Theorem 1, agent i has exactly two neighbors for all $i \in \{3, \ldots, N\}$. Let i_α and i_β be the indices for neighbors of agent i, i.e., $i_\alpha, i_\beta \in \mathcal{N}_i$, $i_\alpha \neq i_\beta$, $i_\alpha < i$ and $i_\beta < i$. Let $V_i(\mathbf{z}) = \phi_i(\mathbf{p}) = \frac{1}{4}(e_{i_\alpha i}^2 + e_{i_\beta i}^2)$, where $\mathbf{z} = [\ldots\ \ \mathbf{z}_{ij}^\top\ \ \ldots]^\top \in \mathbb{R}^{2|\mathcal{E}|}$. By taking the derivative of V_i, we have

$$\dot{V}_i = -\cos\theta \|e_{i_\alpha i}\mathbf{z}_{i_\alpha i} + e_{i_\beta i}\mathbf{z}_{i_\beta i}\|^2$$

$$+\underbrace{(e_{i_\alpha i}\mathbf{z}_{i_\alpha i}^\top \mathbf{u}_{i_\alpha} + e_{i_\beta i}\mathbf{z}_{i_\beta i}^\top \mathbf{u}_{i_\beta})}_{\triangleq h_i(\mathbf{z}(t))}, \tag{19}$$

which is similar to $\dot{V}_3$ in (17). Thus, if $\|\mathbf{u}_{i_\alpha}\|$ and $\|\mathbf{u}_{i_\beta}\|$ are bounded by exponentially decaying functions, then we can apply the same logic used in the proof of Lemma 1 and Theorem 2.

To show that all of the squared-distance errors converge to zero, let us first consider a formation produced by a subgraph $\mathcal{G}_s$ such that $\mathcal{G}_s = (\mathcal{V}_s, \mathcal{E}_s)$, $\mathcal{V}_s = \{1,\ldots,s\} \subseteq \mathcal{V}$, $\mathcal{E}_s = \{(j,i) \in \mathcal{E} \colon i \in \mathcal{V}_s\} \subseteq \mathcal{E}$. For $s = 3$, we showed that e_{ji} is bounded by an exponentially decaying function for all $(j,i) \in \mathcal{E}_s$ in Section 3.. To use induction on s, let us assume that e_{ji} is bounded by an exponentially decaying function for all $(j,i) \in \mathcal{E}_s$ for $s = k-1$. For $s = k$, $\dot{V}_k$ is given by (19) with $i = k$. We assumed that $k_\alpha < k$ and $k_\beta < k$. Hence, $\mathbf{u}_{k_\alpha}$ and $\mathbf{u}_{k_\beta}$ consist of $\{e_{ji}\}$ such that $(j,i) \in \mathcal{E}_{k-1}$. Therefore, from the assumption, $e_{k_\alpha k}$ and $e_{k_\beta k}$ are also bounded by exponentially decaying functions, which means that e_{ji} is bounded by an exponentially decaying function for all $(j,i) \in \mathcal{E}_s$ and for all $s \in \{3,\ldots,N\}$.

Remark 1: We assumed that the inequalities in (3)–(5) hold for three-agent systems. Likewise, we need to assume the following inequalities

$$\|\mathbf{p}_{i_\alpha}^* - \mathbf{p}_i^*\| < \|\mathbf{p}_{i_\beta}^* - \mathbf{p}_i^*\| + \lim_{t\to\infty}\|\mathbf{p}_{i_\alpha}(t) - \mathbf{p}_{i_\beta}(t)\|,$$
$$\|\mathbf{p}_{i_\beta}^* - \mathbf{p}_i^*\| < \|\mathbf{p}_{i_\alpha}^* - \mathbf{p}_i^*\| + \lim_{t\to\infty}\|\mathbf{p}_{i_\alpha}(t) - \mathbf{p}_{i_\beta}(t)\|,$$
$$\lim_{t\to\infty}\|\mathbf{p}_{i_\alpha}(t) - \mathbf{p}_{i_\beta}(t)\| < \|\mathbf{p}_{i_\beta}^* - \mathbf{p}_i^*\| + \|\mathbf{p}_{i_\alpha}^* - \mathbf{p}_i^*\|.$$

Remark 2: Any acyclic minimally persistent graph with at least four vertices is not *globally rigid* in $\mathbb{R}^2$. Therefore, we are not free from the flip ambiguity which may result in different realizations [4]. Therefore, convergence of $\mathbf{z}$ to $\mathcal{D}_{\mathbf{z}^*}$ may not imply convergence of $\mathbf{p}$ to $\mathcal{D}_{\mathbf{p}^*}$. However, if the initial realization is close enough to the desired formation, we have the same conclusion. An intuitive solution to solve the flip ambiguity is proposed by Kang and Ahn [14], but their algorithm requires more information to get rid of such an ambiguity.

5. FORMATIONS WITH MOVING LEADER

In the preceding discussions, the leader agent does not move on because it does not have any neighbor accompanying the distance constraint. However, we may want to drive the leader to move from the initial location $\hat{\mathbf{p}} \in \mathbb{R}^2$ to the desired location $\bar{\mathbf{p}} \in \mathbb{R}^2$. In that regard, let us assume that there exists a velocity profile $\mathbf{v}(t)$ such that

$$\mathbf{v}(t) = \begin{cases} \mathbf{w}(t), & t \in [t_0, t_f], \quad t_f < \infty, \\ 0, & \text{otherwise}, \end{cases}$$

where $\int_{t_0}^{t_f} \mathbf{w}(t)\,\mathrm{d}t = \bar{\mathbf{p}} - \hat{\mathbf{p}}$, and $\mathbf{w}(t)$ is piecewise continuous in t. We want to know what happens if we apply the velocity profile to the leader agent. For simplicity, we only consider the three-agent case with the problem setup in Section 3..

We assign $\mathbf{v}$ to $\mathbf{u}_1$ in (11) instead of $\mathbf{0}$. Then, we have

$$\begin{aligned}\dot{V}_3 &= e_{13}\mathbf{z}_{13}^\top(\mathbf{v} - Q(e_{13}\mathbf{z}_{13} + e_{23}\mathbf{z}_{23})) \\ &\quad + e_{23}\mathbf{z}_{23}^\top(e_{12}\mathbf{z}_{12} - Q(e_{13}\mathbf{z}_{13} + e_{23}\mathbf{z}_{23})) \\ &= -\cos\theta\|e_{13}\mathbf{z}_{13} + e_{23}\mathbf{z}_{23}\|^2 \\ &\quad + \underbrace{e_{13}\mathbf{z}_{13}^\top\mathbf{v} + e_{23}e_{12}\mathbf{z}_{23}^\top\mathbf{z}_{12}}_{\triangleq h(\mathbf{z}(t))}.\end{aligned}$$

Since $\mathbf{v}$ becomes zero in a finite time t_f, the whole systems can be interpreted as the same in Section 3. with different time origin. As a consequence, the finite motion of the leader agent does not affect the analysis, so every squared-distance error converges to 0, and we achieve the desired formation.

6. SIMULATIONS AND EXPERIMENTS

6.1. Simulations

We conducted some simulations supporting our results. Fig. 6 shows that the agents break away from the line configuration for $\mathbf{z}_0 \in \mathcal{C}_2 \setminus \mathcal{U}_3$. We assigned 0.3 to each desired inter-agent distance and $\pi/6$ to θ. To simulate an extreme case, we used an initial condition $[0,\ \ 0,\ \ -0.4,\ \ 0,\ \ -0.2,\ \ 0]^\top$ for $\mathbf{p}(0)$ so that the initial velocity of agent 3 became 0. Nevertheless, they immediately break away from the line configuration because the movement of agent 2 due to nonzero error e_{12} make $\mathbf{u}_3$ nonzero.

Fig. 7 shows that our results are applicable to the formations having more than three agents. Desired distances are as follows:

$$\begin{aligned}&d_{12} = 0.3, \quad d_{13} = 0.5, \quad d_{23} = 0.4, \quad d_{24} = 0.5, \\ &d_{34} = 0.5, \quad d_{25} = 0.5, \quad d_{45} = 0.5.\end{aligned}$$

Note that the final formation is flipped over in Fig. 8(a) compared to Fig. 7(a) as mentioned in Remark 2 even though every squared-distance error converges to 0.

In Fig. 9, the leader agent moves on with finite velocity. As soon as the leader stops, the squared-distance errors start to converge to zero.

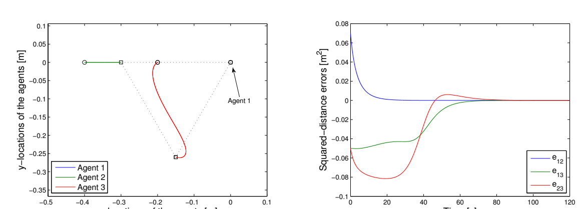

(a) Trajectories and final formation. (b) Corresponding distance errors.

Fig. 6. 3-agent formation initially located in collinear position.

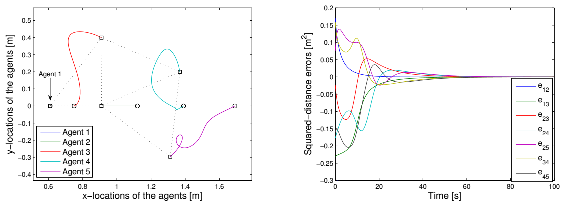

(a) Trajectories and final formation. (b) Corresponding distance errors.

Fig. 7. 5-agent formation initially located in collinear position.

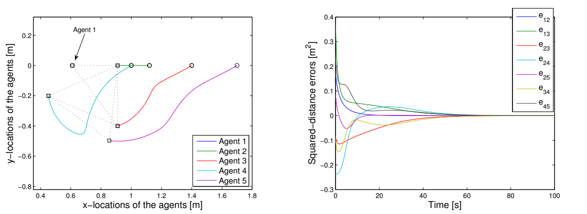

(a) Trajectories and final formation. (b) Corresponding distance errors.

Fig. 8. 5-agent flipped over formation.

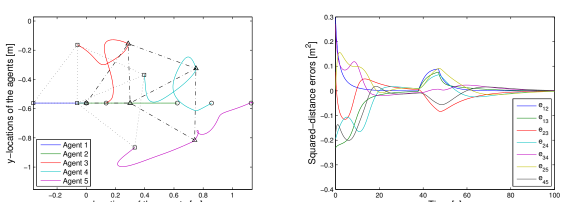

(a) Trajectories and final formation. (b) Corresponding distance errors.

Fig. 9. Moving formation, $\mathbf{w}(t) = [-39/1000 \quad 0]^\top$, $t_0 = 37.7$, $t_f = 47$.

6.2. Experiments

We conducted experiments by means of a group of two-wheeled mobile robots named e-puck which is illustrated in Fig. 10(a). The user can assign the velocity of each wheel to maneuver the robot motion. Although an e-puck robot has two wheels, the motion of the robot can be reduced to the motion of a unicycle. For example,

$$\dot{x}_i = v_i \cos\phi_i, \tag{20}$$

$$\dot{y}_i = v_i \sin\phi_i, \tag{21}$$

$$\dot{\phi}_i = \omega_i, \tag{22}$$

where $\mathbf{p}_i = [x_i \ \ y_i]^\top$, ϕ_i is the heading angle of robot i with respect to x-axis, and v_i and ω_i are the linear and angular velocity of robot i, respectively. In the unicycle model, a challenging problem in implementing the control law in (9) is that (20)–(22) do not match with the single integrator dynamics. In the literature, some researchers control a point in front of the unicycle instead of the exact location of the unicycle to achieve the single integrator model by using feedback linearization [6].

Instead, we control the location of the mobile robot, and make the motion of e-puck robot approximate the motion of single integrator. Let $\angle\mathbf{u}_i$ denote the angle of the vector $\mathbf{u}_i \in \mathbb{R}^2$ with respect to the x-axis. If we can assign $v_i = \|\mathbf{u}_i\|$ with $\angle\mathbf{u}_i - \phi_i = 0$, then the robot will follow the trajectory $\mathbf{p}_i(t)$ obtained from (1) and (9). However, $\angle\mathbf{u}_i - \phi_i = 0$ is not achievable in actual implementation. Therefore, by making $\angle\mathbf{u}_i - \phi_i$ sufficiently small, we achieve the approximation.

In the first experiment, we used initial conditions similar to those used in the simulation illustrated in Fig. 7. Fig. 11 shows the results of the experiment with a group of 5 robots. They were initially located in a line configuration denoted by circles in Fig. 11(a). The snapshots of the group are posted in Fig. 12. After 60 s, the formation of the group is very close to the desired formation shape, and the squared-distance errors are close to 0.

Next, we conducted an experiment with a moving leader of which the velocity profile is

$$\mathbf{v}(t) = \begin{cases} [-39/1000 \quad 0]^\top, & t \in [37.7, 47], \\ \mathbf{0}, & \text{otherwise}. \end{cases}$$

While the leader moves with nonzero velocity, the squared-distance errors do not converge to 0 (see Fig. 13(b)). However, after that the leader stops, the squared-distance errors ultimately converge to 0. The snapshots of the group are posted in Fig. 14.

(a) A two-wheeled mobile robot. (b) A group of mobile robots.

Fig. 10. Mobile robot platform.

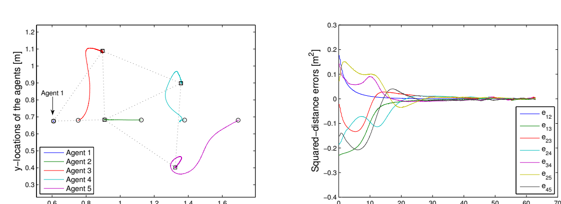

(a) Trajectories and final formation. (b) Corresponding distance errors.

Fig. 11. Experimental results of 5 agent group.

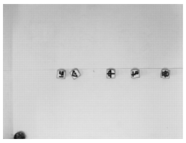
(a) $t = 0$.
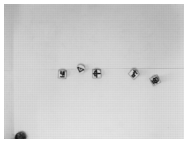
(b) $t = 5$.
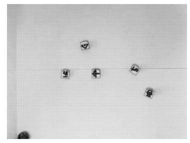
(c) $t = 10$.
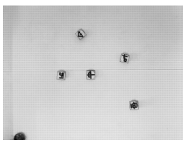
(d) $t = 15$.
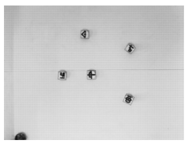
(e) $t = 20$.
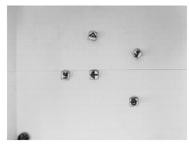
(f) $t = 60$.

Fig. 12. Experimental results of 5 agent group.

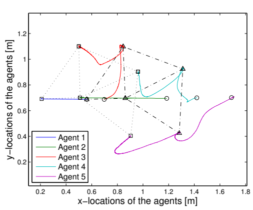

(a) Trajectories and final formation.
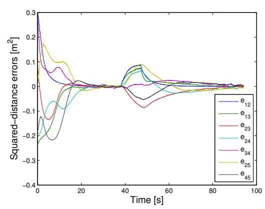

(b) Corresponding distance errors.

Fig. 13. Experimental results of 5 agent group.

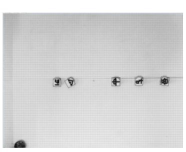
(a) $t = 0$.
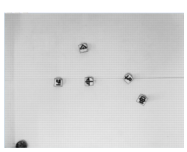
(b) $t = 10$.
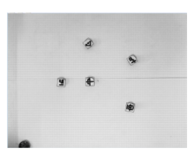
(c) $t = 35$.
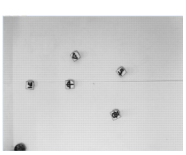
(d) $t = 47$.
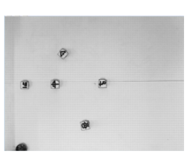
(e) $t = 55$.
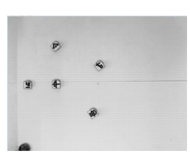
(f) $t = 90$.

Fig. 14. Experimental results of 5 agent group with moving leader.

7. CONCLUSIONS

We proposed a control law for the distance-based formation control problems on which the corresponding formations are represented by acyclic minimally persistent graphs. The control law was devised in the spirit of the generalization of the steepest descent gradient control law to one containing non-steepest direction. We first analyzed the basic triangular formation, and then extended the results to acyclic minimally persistent formations. We also considered the moving leader case without loss of generality, although the motion of the leader is limited. To verify the theory, we used a mobile robot platform consisting of e-puck robots. Although, the motion of the two-wheeled mobile robot is not modeled by a single integrator, we can approximate the motion so that it follows a trajectory generated from the single integrator.

Unfortunately, we are not sure whether or not our results could be applied to more general formations such as cycle formations or persistent formations without minimality. Hence, extending our results to more general formations will be important future work.

APPENDIX A

We are going to show that at least one of the eigenvalues of $J_{\mathbf{f}}$ has a strictly positive real part by investigating the eigenvalues of $K_{\mathbf{f}}$. Let

$$\lambda I_4 - K_{\mathbf{f}} = \begin{bmatrix} \lambda I_2 + Q(Z_{13} + e_{13} I_2) & Q(Z_{23} + e_{23} I_2) \\ Q(Z_{13} + e_{13} I_2) & \lambda I_2 + Q(Z_{23} + e_{23} I_2) \end{bmatrix}.$$

By eliminations, we have

$$(\lambda I_4 - K_{\mathbf{f}})_{\mathrm{ref}} = \begin{bmatrix} \lambda I_2 + Q(Z_{13} + e_{13} I_2 + Z_{23} + e_{23} I_2) & Q(Z_{23} + e_{23} I_2) \\ 0_{2\times 2} & \lambda I_2 \end{bmatrix}. \tag{A.1}$$

From (A.1), it is obvious that two eigenvalues of $K_{\mathbf{f}}$ are 0, and the others are the eigenvalues of $L_{\mathbf{f}}$, where

$$L_{\mathbf{f}} = -Q(Z_{13} + e_{13} I_2 + Z_{23} + e_{23} I_2).$$

We are going to show that $L_{\mathbf{f}}$ has at least one eigenvalue whose real part is strictly positive. Since $e_{13}\mathbf{z}_{13} + e_{23}\mathbf{z}_{23} = \mathbf{0}$ for $\mathbf{z} \in \mathcal{U}_3$, $Z_{23} = (e_{13}/e_{23})^2 Z_{13}$. Hence,

$$L_{\mathbf{f}} = -2Q \times \begin{bmatrix} x_{13}^2 \left(\frac{e_{13}^2 + e_{23}^2}{e_{23}^2}\right) + \frac{e_{13} + e_{23}}{2} & x_{13} y_{13} \left(\frac{e_{13}^2 + e_{23}^2}{e_{23}^2}\right) \\ x_{13} y_{13} \left(\frac{e_{13}^2 + e_{23}^2}{e_{23}^2}\right) & y_{13}^2 \left(\frac{e_{13}^2 + e_{23}^2}{e_{23}^2}\right) + \frac{e_{13} + e_{23}}{2} \end{bmatrix}$$

and

$$\det L_{\mathbf{f}} = (e_{13} + e_{23}) \left(\frac{2e_{13}^2 \|\mathbf{z}_{13}\|^2 + 2e_{23}^2 \|\mathbf{z}_{13}\|^2}{e_{23}^2} + e_{13} + e_{23} \right),$$

where $\mathbf{z}_{ij} = [x_{ij} \quad y_{ij}]^\top$. From the fact that $e_{13}^2 \|\mathbf{z}_{13}\|^2 = e_{23}^2 \|\mathbf{z}_{23}\|^2$ and $\|\mathbf{z}_{13} - \mathbf{z}_{23}\| = d_{12}$ for all $\mathbf{z} \in \mathcal{U}_3$, we have

$$\begin{aligned} \det L_{\mathbf{f}} &= (e_{13} + e_{23})(2\|\mathbf{z}_{13}\|^2 + 2\|\mathbf{z}_{23}\|^2 + e_{13} + e_{23}) \\ &= (e_{13} + e_{23})(-d_{13}^2 - d_{23}^2 + 3\|\mathbf{z}_{13} - \mathbf{z}_{23}\|^2 + 6\mathbf{z}_{13}^\top \mathbf{z}_{23}) \\ &= (e_{13} + e_{23})(-d_{13}^2 - d_{23}^2 + 3d_{12}^2 + 6\mathbf{z}_{13}^\top \mathbf{z}_{23}). \end{aligned}$$

Similarly,

$$
\begin{aligned}
&\operatorname{trace} L_{\mathbf{f}} \\
&= -\left(2x_{13}^2 \frac{e_{13}^2+e_2^{23}}{e_{23}^2} + e_{13} + e_{23}\right)\cos\theta \\
&\quad + 2x_{13}y_{13}\frac{e_{13}^2+e_{23}^2}{e_{23}^2}\sin\theta - 2x_{13}y_{13}\frac{e_{13}^2+e_{23}^2}{e_{23}^2}\sin\theta \\
&\quad - \left(2y_{13}^2 \frac{e_{13}^2+e_{23}^2}{e_{23}^2} + e_{13} + e_{23}\right)\cos\theta \\
&= 2\left(-(e_{13}+e_{23}) - \frac{\|\mathbf{z}_{13}\|^2\left(e_{13}^2+e_{23}^2\right)}{e_{23}^2}\right)\cos\theta \\
&= 2(-e_{13}-e_{23}-\|\mathbf{z}_{13}\|^2-\|\mathbf{z}_{23}\|^2)\cos\theta \\
&= 2(d_{13}^2+d_{23}^2-2\|\mathbf{z}_{13}-\mathbf{z}_{23}\|^2-4\mathbf{z}_{13}^\top\mathbf{z}_{23})\cos\theta \\
&= 2(d_{13}^2+d_{23}^2-2d_{12}^2-4\mathbf{z}_{13}^\top\mathbf{z}_{23})\cos\theta.
\end{aligned}
$$

Cao *et al.* proved that $e_{13}+e_{23}<0$ for $\mathbf{z}\in\mathcal{U}_3$ [5, Lemma 5]. Therefore, If $-d_{13}^2-d_{23}^2+3d_{12}^2+6\mathbf{z}_{13}^\top\mathbf{z}_{23}>0$, then $\det L_{\mathbf{f}}<0$, which means that the eigenvalues of $L_{\mathbf{f}}$ have opposite signs because $\det L_{\mathbf{f}}$ is the product of all eigenvalues of $L_{\mathbf{f}}$. On the other hand, if

$$2d_{12}^2+4\mathbf{z}_{13}^\top\mathbf{z}_{23}\leq\frac{2}{3}(d_{13}^2+d_{23}^2),$$

then

$$\operatorname{trace} L_{\mathbf{f}}\geq\frac{2}{3}\cos\theta(d_{13}^2+d_{23}^2),$$

which means that at least one of the eigenvalues of $L_{\mathbf{f}}$ has a positive real part because $\operatorname{trace} L_{\mathbf{f}}$ is the sum of all eigenvalues of $L_{\mathbf{f}}$. Accordingly, we can conclude that $\mathcal{U}_3$ is unstable.

REFERENCES

[1] H. Yamaguchi, T. Arai, and G. Beni, "A distributed control scheme for multiple robotic vehicles to make group formations," *Robotics and Autonomous Systems*, vol. 36, no. 4, pp. 125–147, 2001. [click]

[2] M. Cao, A. S. Morse, C. Yu, B. D. O. Anderson, and S. Dasgupta, "Controlling a triangular formation of mobile autonomous agents," *Proceedings of the 46th IEEE Conference on Decision and Control*, Dec. 2007, pp. 3603–3608. [click]

[3] S. Kalantar and U. R. Zimmer, "Distributed shape control of homogeneous swarms of autonomous underwater vehicles," *Autonomous Robots*, vol. 22, no. 1, pp. 37–53, 2007. [click]

[4] B. D. O. Anderson, C. Yu, B. Fidan, and J. M. Hendrickx, "Rigid graph control architectures for autonomous formations," *IEEE Control Systems Magazine*, vol. 28, no. 6, pp. 48–63, 2008. [click]

[5] M. Cao, B. D. O. Anderson, A. S. Morse, and C. Yu, "Control of acyclic formations of mobile autonomous agents," *Proceedings of the 47th IEEE Conference on Decision and Control*, pp. 1187–1192, Dec. 2008. [click]

[6] W. Ren and N. Sorensen, "Distributed coordination architecture for multi-robot formation control," *Robotics and Autonomous Systems*, vol. 56, no. 4, pp. 324–333, 2008. [click]

[7] L. Krick, M. E. Broucke, and B. A. Francis, "Stabilisation of infinitesimally rigid formations of multi-robot networks," *International Journal of Control*, vol. 82, no. 3, pp. 423–439, 2009. [click]

[8] C. Yu, B. D. O. Anderson, S. Dasgupta, and B. Fidan, "Control of minimally persistent formations in the plane," *SIAM Journal on Control and Optimization*, vol. 48, no. 1, pp. 206–233, 2009. [click]

[9] F. Dörfler and B. Francis, "Geometric analysis of the formation problem for autonomous robots," *IEEE Transactions on Automatic Control*, vol. 55, no. 10, pp. 2379–2384, 2010. [click]

[10] M. Cao, A. S. Morse, C. Yu, B. D. O. Anderson, and S. Dasgupta, "Maintaining a directed, triangular formation of mobile autonomous agents," *Communications in Information and Systems*, vol. 11, no. 1, pp. 1–16, 2011. [click]

[11] K.-K. Oh and H.-S. Ahn, "Formation control of mobile agents based on inter-agent distance dynamics," *Automatica*, vol. 47, no. 10, pp. 2306–2312, 2011. [click]

[12] T. H. Summers, C. Yu, S. Dasgupta, and B. D. O. Anderson, "Control of minimally persistent leader-remote-follower and coleader formations in the plane," *IEEE Transactions on Automatic Control*, vol. 56, no. 12, pp. 2778–2792, 2011. [click]

[13] K.-K. Oh and H.-S. Ahn, "Distance-based undirected formations of single-integrator and double-integrator modeled agents in *n*-dimensional space," *International Journal of Robust and Nonlinear Control*, vol. 24, no. 12, pp. 1809–1820, 2014. [click]

[14] S.-M. Kang and H.-S. Ahn, "Global convergence of formation in multi-agent systems without global reference frame," *Proceedings of the 2015 IEEE International Symposium on Intelligent Control*, Sep. 2015, pp. 646–651. [click]

[15] K.-K. Oh, M.-C. Park, and H.-S. Ahn, "A survey of multi-agent formation control," *Automatica*, vol. 53, pp. 424–440, 2015. [click]

[16] J. Yan, X. Yang, X.-T. Luo, X.-P. Guan, and C.-C. Hua, "Wireless network based formation control for multiple agents," *International Journal of Control, Automation and Systems*, vol. 12, no. 2, pp. 415–421, 2014. [click]

[17] Y. Jia and W. Zhang, "Distributed adaptive flocking of robotic fish system with a leader of bounded unknown input," *International Journal of Control, Automation and Systems*, vol. 12, no. 5, pp. 1049–1058, 2014. [click]

[18] B. S. Park and S. J. Yoo, "Adaptive leader-follower formation control of mobile robots with unknown skidding and slipping effects," *International Journal of Control, Automation and Systems*, vol. 13, no. 3, pp. 587–594, 2015. [click]

[19] B. Hendrickson, "Conditions for unique graph realizations," *SIAM Journal on Computing*, vol. 21, no. 1, pp. 65–84, 1992. [click]

[20] J. M. Hendrickx, B. D. O. Anderson, J.-C. Delvenne, and V. D. Blondel, "Directed graphs for the analysis of rigidity and persistence in autonomous agent systems," *International Journal of Robust and Nonlinear Control*, vol. 17, no. 10-11, pp. 960–981, 2007. [click]

[21] C. Yu, J. M. Hendrickx, B. Fidan, B. D. O. Anderson, and V. D. Blondel, "Three and higher dimensional autonomous formations: Rigidity, persistence and structural persistence," *Automatica*, vol. 43, no. 3, pp. 387–402, 2007. [click]

[22] H. K. Khalil, *Nonlinear Systems*, 3rd ed., Prentice Hall, NJ, 2002.

Myoung-Chul Park received the B.S. degree in electronics engineering from Chungnam National University, Daejeon, Korea, in 2011, and the M.S. degree in information and mechatronics from Gwangju Institute of Science and Technology (GIST), Gwangju, Korea, in 2013. He is currently working toward the Ph.D. degree in mechatronics at GIST. His research interests include decentralized control of multi-agent systems and localization of sensor networks.

Hyo-Sung Ahn received the B.S. and M.S. degrees in astronomy from Yonsei University, Seoul, Korea, in 1998 and 2000, respectively, the M.S. degree in electrical engineering from the University of North Dakota, Grand Forks, in 2003, and the Ph.D. degree in electrical engineering from Utah State University, Logan, in 2006. Since July 2007, he has been with the School of Mechatronics, Gwangju Institute of Science and Technology (GIST), Gwangju, Korea. He is currently Associate Professor and Dasan Professor. Before joining GIST, he was a Senior Researcher with the Electronics and Telecommunications Research Institute, Daejeon, Korea. He is the author of the research monograph Iterative Learning Control: Robustness and Monotonic Convergence for Interval Systems (Springer-Verlag, 2007). His research interests include distributed control, learning control, network localization, and autonomous navigation systems.